


Article

Rice Derivatives in Hair Protecting

Marisanna Centini ^{1,2,*}, Giulia Signori ¹ , Fabrizio Francescon ³, Fumi Tsuno ⁴, Tomoki Oguro ⁴ and Cecilia Anselmi ^{1,2}

¹ Dipartimento di Biotecnologie, Chimica e Farmacia, Via Aldo Moro 2, 53100 Siena, Italy; signori4@student.unisi.it (G.S.); cecilia.anselmi@unisi.it (C.A.)

² Unicosmesi Srl, Piazza del Sale 9, 53100 Siena, Italy

³ FEELCOSMETIC S.R.L., Via Vecchia Aretina, 93/95, Montalto, 52019 Arezzo, Italy; info@fabriziofrancescon.it

⁴ Tsuno Rice Fine Chemical Co., Ltd., Wakayama 649-7194, Japan; fumi@tsuno.co.jp (F.T.); oguro.tomoki@tsuno.co.jp (T.O.)

* Correspondence: marisanna.centini@unisi.it

Abstract: The research was carried out on a hair conditioner containing the following rice derivatives individually: rice germ oil, rice germ oil GX-N, and riceterol esters. To evaluate the protective efficacy of the three active ingredients chosen, the following techniques were used: FT-IR, SEM, stress-strain test, and polarized light microscopy analysis. The tests were carried out on natural Caucasian hair. The methodologies were found to be suitable for the evaluation and led to interesting results: the selected ingredients showed good properties in improving the hair. The conditioners containing the active ingredients restored the properties of the hair even when subjected to stress such as irradiation. In this case, the most effective was the rice germ oil GX-N.

Keywords: hair conditioner; rice derivatives; hair protection; hair evaluation

1. Introduction

The hair fiber contains three different units (structures): the cuticle, cortex, and medulla. All of them are constituted of dead cells, which mainly contain the keratin protein. The cuticle is a thick protective coating, localized on the surface, consisting of layers of flat overlapping, scale-like structures directed toward the tip of the hair. Each cell of the cuticle is composed of three layers: the A layer and the exocuticle with a high cystine content and the endocuticle with a low cystine content. Each cell of the cuticle is coated by the epicuticle, a thin membrane constituted of proteins and lipids. The cell membrane complex (CMC), consisting of a lipid bilayer flanked by protein layers, separates the cuticle cells. The cuticle layers surround the cortex, which contains the major part of the fiber mass. The cortex consists of spindle-shaped cells that are aligned along the fiber axis; the cortex cells contain the fibrous proteins of the hair. Cortical cells are formed of macrofibrils, which are composed of intermediate filaments (or microfibrils) embedded in a matrix rich in cystine. The medulla is a porous region located near the center of the fiber [1].

UV radiation and solar radiation cause various photochemical reactions ranging from the discoloration of the hair to the photodegradation of disulphide bonds and these effects are greater on the distal parts, then on the proximal ones, where there is a greater quantity of cysteic acid [2,3]. It is also known that irradiation has an important effect on the tensile properties of human hair, i.e., the tensile properties of the fiber decrease upon exposure to light, since the lower levels of cysteine and the generation of cysteic acid reduce the stabilizing effect of the disulphide bonds. Furthermore, the chemical alteration of the aromatic nuclei of tyrosine and phenylalanine, as well as the decarboxylation of amino acids, contributes to the reduction in the tensile properties. Then, the tensile properties can be used to evaluate the photoprotection of the hair [4].

Hair structure characterization and the evaluation of its physical and mechanical properties are essential for the development of hair care products. The evaluation of the



Citation: Centini, M.; Signori, G.; Francescon, F.; Tsuno, F.; Oguro, T.; Anselmi, C. Rice Derivatives in Hair Protecting. *Cosmetics* **2023**, *10*, 163. <https://doi.org/10.3390/cosmetics10060163>

Academic Editor: Kazuhisa Maeda

Received: 5 October 2023

Revised: 6 November 2023

Accepted: 20 November 2023

Published: 29 November 2023



Copyright: © 2023 by the authors. Licensee MDPI, Basel, Switzerland. This article is an open access article distributed under the terms and conditions of the Creative Commons Attribution (CC BY) license (<https://creativecommons.org/licenses/by/4.0/>).

effectiveness of hair care products can be carried out *in vitro* with instrumental techniques generally endowed with a high sensitivity [5–7]. The advantages of these techniques, compared with subjective evaluation (test in use, salon test), are (i) no need for a panel of volunteers, (ii) the use of standardized hair strands, (iii) quick evaluation, and (iv) the use of standardized test conditions. Various techniques are used [5–7].

Microscopy and image analyses are used to study the structure of the hair, the penetration of materials, and the presence of substances deposited on the hair and to evaluate its damage [6]. Various studies have been performed by fluorescence microscopy (conventional and confocal) [6,8], by scanning electron microscopy (SEM) [7,9,10], by transmission electron microscopy (TEM) [7,11,12], and by atomic force microscopy (AFM) [13,14].

The same evaluations can be carried out through spectroscopic techniques. Pavani et al. [15] applied fluorescence spectroscopy for the assessment of hair photo-induced damage. Fourier transform infrared spectroscopy can be applied for the detection of molecules that bind to the hair, for the study of structural and morphological variations of the hair due to bleaching and/or coloring and for the study of the state of hydration induced by the application of a conditioning product [11,16].

Raman spectroscopy can be applied for various types of investigations such as modification of the hair structure caused by chemical treatments [17], by ageing [17], by UV radiation [18], and by penetration of amino acids, peptides, and protein hydrolysates [19].

The diffuse reflectance is used to measure the luminosity and color of the hair before and after the treatment with hair care products [20]. The detection and quantification of substances absorbed by the hair such as silicones and metals can be performed by atomic emission or optical emission inductively coupled plasma spectroscopy (ICP-AES, ICP-OES) [21,22]. Thermal analysis can be applied for the characterization of the keratin of the hair [23] and for the study of the influence of treatments on its structure [24,25]. The most used techniques are thermogravimetry (TG), differential thermogravimetry (DTG), differential thermal analysis (DTA), differential scanning calorimetry (DSC), and thermochemical analysis (TMA) [7].

Others techniques that can be used in the study of the hair are (i) gel-permeation chromatography and gel-filtration chromatography for the evaluation of absorption of substances such as cationic polymers, peptides, and amino acids [26,27] and (ii) electrophoresis to evaluate the modification of the hair protein composition due to its degradation or to chemical treatments [7]. Cuticle damage due to bleaching or frequent washing has been evaluated by acoustic emission analysis [28] and by laser scattering analysis [29], respectively.

Other evaluations, such as the measurement of tensile strength, of elasticity, and of combability, have been done using a dynamometer [5,30].

The use of rice derivatives in food, pharmaceuticals, and cosmetics has been known for a long time. Their effectiveness, especially on the skin, has been the subject of many publications, and more recently, also their application on the hair has assumed great importance [31–34]. Innovative technologies have caused it to be possible to obtain many components derived from both bran and germ rice, and then these can be applied in various fields including the cosmetics sector, as single active raw materials [35,36].

In this work, three rice derivatives, rice germ oil PRO-15 (PRO-15), rice germ oil GX-N (GX-N), and riceterol esters (RSEs), were chosen to evaluate their application properties on the hair, not yet investigated.

They were added at a concentration of 1% in a hair conditioner product. It was a rinsing conditioner formulated as an oil-in-water emulsion containing cationic derivatives and a small percentage of silicone derivatives.

For these three active ingredients, emollient, moisturizing, and anti-aging effects on the skin have been highlighted [37,38]. PRO-15 is a refined rice germ oil that has good temperature and oxidation stabilities in comparison with other oils (soy, sunflower, cotton, corn..), and it also has antioxidant properties due to the high content of unsaponifiables ($\geq 6\%$) rich in tocopherols, tocotrienols, γ -oryzanol, and phytosterols. Rice germ oil has a superior quality with respect to rice bran oil due to the higher γ -oryzanol content, which

offers increased antioxidant activity [39]. Rice germ oil GX-N has a higher γ -oryzanol content than normal rice germ oil (about 30%). Riceterol esters are ingredients obtained from the by-products of the rice bran oil refining process. They appear as a pasty oil at room temperature, and it is rich in esters of phytosterols, triterpene alcohols, and fatty acids. These compounds show high water retention and emollient effects on the skin [38]. Preliminary tests have highlighted a possible prevention effect on hair damage (Oguro et al., unpublished data). The literature shows that rice derivatives are safe as dermatological and cosmetic ingredients [31,33–35]. The risk assessment for humans toward exposure to rice derivatives has shown low or no toxicity in various toxicological tests [31].

The aim of this work was to evaluate the protective effect on the hair of the three formulations by comparison with a reference (control) that lacked the three active ingredients used individually. The techniques used for the evaluation, Fourier transform infrared spectroscopy (FT-IR), scanning electron microscopy (SEM), a stress–strain test, and polarized light microscopy analysis, are easily accessible and among the most used to highlight any change in the characteristics of the hair.

2. Materials and Methods

2.1. Materials

Natural black hair tresses (33 cm in length) were provided by Azienda Tricologica Italiana Srl (Rome, Italy). Rice germ oil PRO-15, rice germ oil GX-N, riceterol esters, and the conditioners were provided by Tsuno Rice Fine Chemicals Co., Ltd. (Wakayama, Japan).

2.2. Hair Treatment

Caucasian hair was chosen because the Asian hair has a larger diameter and a circular geometry, while the African hair is irregular in diameter and has an elliptical section. The Caucasian hair has a diameter and a shape of intermediate section [1].

The 33 cm long virgin hair tresses (i.e., hair without chemical and physical damage) were used. First, the hair lock (about 40.00 g) was washed: warm water (approximately 30 °C) and 2.10 g of shampoo (ingredients: Aqua, Tea-Laureth Sulfate, Cocamidopropyl Betaine, Propylene Glycol, Malva Sylvestris Extract, Parfum, 1,2-Hexanediol, Sodium EDTA, Citric Acid, Sodium Benzoate, Potassium Sorbate) were put in a beaker, and subsequently, the hair lock was added and the mixture was left under stirring for one minute. After that, the hair lock was rinsed under warm running water and left air-dried.

After this operation, the samples were prepared. Five locks of hair of about 1.00 g each were prepared, and four of these were treated with about 1.00 g of the conditioners (the other strand represented the untreated hair). Three locks of hair were treated with the pure active ingredients with an amount equivalent to that contained in 1.00 g of conditioner (0.01 g). The product was carefully applied from the upper part toward the tip, then it was allowed to be in contact with the hair without manipulation for 1 min. After that, the hair treated with the four conditioners and with the pure active ingredients was washed only with warm running water for about 1 min, then it was air-dried and stored wrapped in aluminum foil for the subsequent experiments.

2.3. FT-IR Analysis

An Agilent Technologies Cary 630 FTIR spectrometer (Agilent Technologies Italia Spa, Milan, Italy) was used to obtain the IR spectra. The MicroLab program was used for data processing. The samples to be registered were placed on the appropriate support (Diamond ATR Sampling Accessory) and recorded using the Agilent MicroLab PC software B.05.3 (Agilent Technologies Italia Spa, Milan, Italy).

The FT-IR spectra were recorded on three parts of the untreated hair (not irradiated and irradiated): the upper part (the proximal part of the hair), the central part, and the lower part (the distal part of the hair). The same spectra were recorded on the hair (not irradiated and irradiated) treated with the four conditioners. Moreover, the FT-IR spectra

were recorded on the pure active ingredients, on the four conditioners, and on the hair treated with the pure active ingredients.

2.4. SEM Analysis

The SEM images were obtained with a scanning electron microscope, Quanta 400 SEM (FEI). The 1 cm long hair pieces were cut with a scalpel, mounted on stubs with copper conductive tape, and sputter coated with gold before the analysis.

The SEM images were recorded on three parts of the untreated hair (not irradiated and irradiated): the upper part (the proximal part of the hair), the central part, and the lower part (the distal part of the hair). Moreover, the images were acquired on the cross-section of the hair and on the knotted hair. The same analyses were performed on the hair treated with the four conditioners.

2.5. Hair Irradiation

The irradiation was carried out according to the International Standard Organization (ISO) 105B02 [40]. The tool used was the Xenon Test Chamber Q-LAB, Q-SUN Mod. Xe-2.

The hair was individually housed on the instrument holder, fixing it at the end with an adhesive. A window was cut out of the holder to allow the complete irradiation of the hair. The operating conditions were as follows: irradiation time, 40 h; power of the xenon lamp, 1800 watts; temperature, 47 °C; and relative humidity, 40%.

The irradiation was performed on the untreated hair and on the hair treated with the various conditioners.

2.6. Stress–Strain Test

The determination of the tensile properties was carried out on the blank (untreated hair), on the hair treated with the various conditioners (control and containing the active ingredients (1% GX-N or PRO-15 or RSEs)), and on all non-irradiated and irradiated samples.

The test was performed using a dynamometer (Hounsfield Test Equipment, Dynamometer type CRE; Machine serial number: H10KS-0074), which was able to obtain the stress–strain curve and tenacity assessment. The dynamometer type CRE (Constant Rate of Extension) was adapted with a software that traced the force/extension curve. This equipment can operate at different constant increase in extension from 5 mm/min to 20 mm/min. The hair fiber diameter was obtained using an optical microscope (PZO MP3, Mod. 2563). The hair fibers could be not less than 10 cm long; 20 hair fibers were needed for the test. At the beginning, we measured the linear mass (LM) of the hair fibers according to the following procedure: (a) from both extremities of each hair fiber, 3–4 mm of hair was taken and placed on a cover glass using Silicon Oil AS4 as a fixative oil (for their immersion) (in theory, cedar oil is used), and then the prepared sample was covered with a cover slip; (b) using the optical microscope and applying the following formula, we calculated the medium apparent diameter (MAD) of the two little pieces of the hair fiber placed in the cover glass.

$$(\text{class1} \times 2) + 1 = \text{AD1}$$

$$(\text{class2} \times 2) + 1 = \text{AD2}$$

$$(\text{AD1} + \text{AD2})/2 = \text{MAD of the hair fiber}$$

class = the unit of the optical microscope;

AD1 = apparent diameter of the first piece of the hair fiber expressed in μm ;

AD2 = apparent diameter of the second piece of the hair fiber expressed in μm ;

MAD = medium apparent diameter of the hair fiber.

Then for each fiber we calculated the LM in Tex according to the following formula:

$$\text{Tex} = \frac{\left(\frac{\text{MAD}}{2}\right)^2 \times 3.14 \times 1.31^*}{1000}$$

*1.31 = specific weight of wool similar to hair fiber.

2.7. Hair Protection Factor (HPF)

The evaluation of the HPF value was performed on hair treated with conditioners containing the various active ingredients.

From the stress–strain curves obtained from each hair, the slopes of the yield region between 15 and 30% elongation were calculated as suggested by Bayak [41,42]. The yield point at 15% elongation was shown to be independent of cross-sectional aberrations and responsive to chemical effects; thus, it served as a convenient reference point for detecting tensile changes in the hair as a result of disulphide rupture [42]. When the hair was extended with a tensile strength tester, the changes in the slope of the stress–strain curve in the yield region correlated well with the amount of ultraviolet radiation to which the hair was exposed. The HPF was determined by applying the following formula, reported by Nacht [2]:

$$\text{HPF} = \frac{(\text{yieldslope nonirradiated} - \text{yieldslope irradiated})_{\text{unprotected hair}}}{(\text{yieldslope nonirradiated} - \text{yieldslope irradiated})_{\text{protected hair}}}$$

unprotected hair: not treated hair;

protected hair: hair treated with conditioner.

2.8. Polarized Light Microscopy Analysis

The analysis was performed on the untreated hair (not irradiated and irradiated) and on the hair (not irradiated and irradiated) treated with the four conditioners.

The test was performed using a BEL-PML-1 trinocular biological polarized light microscope with a 20× objective. For visualization with this technique, a portion of a hair was cut and arranged in a cover glass with mineral oil. Oil immersion decreased the polarization aberrations due to air–glass interfaces between the sample and the lenses [43]. The evaluation was performed in a portion of about 7/8 cm of three hairs of each sample. The measurement of the diameter was taken from the proximal portion. The evaluation of the detected colors was conducted by making a comparison with the optimal theoretical colors, corresponding to their respective diameters. The average diameter evaluated under a polarized light microscope was around 58–95 μm for not-irradiated hairs and 58–87 μm for irradiated hairs. It should be noted that the colors in this frequency range could be altered by the presence of the silicone included in the formula.

2.9. Statistical Analysis

The data were analyzed by ANOVA and Dunnett's test. Statistical significance was accepted at a level of $p < 0.05$.

3. Results and Discussion

3.1. FT-IR Analysis

Recently, spectroscopy is proving to be a good tool for evaluating the effects of treatments that are harmful to the hair or to the protective effect of cosmetics [15]. FT-IR imaging analysis has found applications in the evaluation of bleaching processes [16], and the ATR FT-IR was useful in identifying cosmetic residue on a single human hair [44]; thus, it was suggested for forensic hair analysis [45,46].

With regard to the untreated hair, the FT-IR spectra recorded on the three analyzed parts of the three used samples did not differ from each other. The overlap of the acquired spectra on the central parts of three human hairs is shown in Figure 1a.

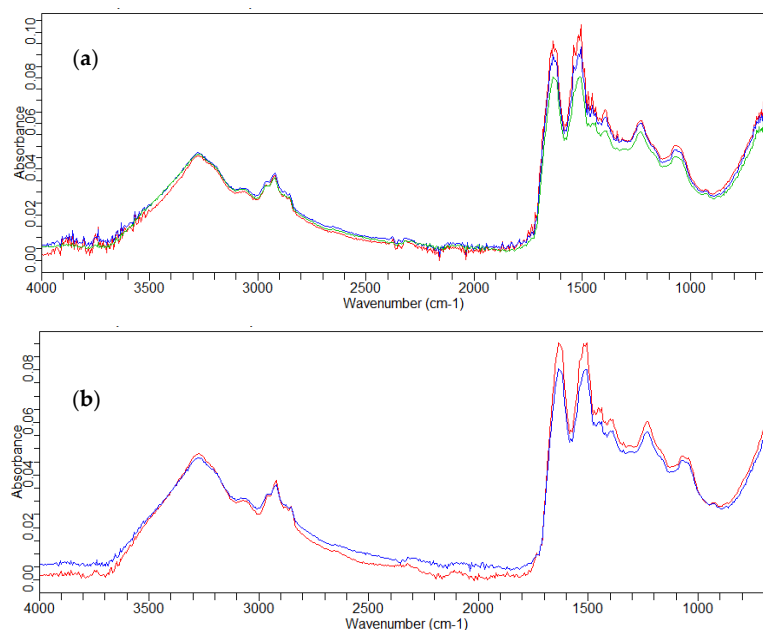


Figure 1. FT-IR spectra of the central parts of untreated hair: (a) overlay of three hairs (— hair 1; — hair 2; — hair 3) and (b) overlay of the hair not irradiated (—) and irradiated (—).

In these spectra we can observe a band at 3278 cm^{-1} , specific of O–H stretching of water together with N–H stretching vibration. The absorption bands at 2957 cm^{-1} and 2920 cm^{-1} were associated with the asymmetric C–H stretching of CH_3 , and the absorption band at 2852 cm^{-1} was attributed to the asymmetric C–H stretching of CH_2 . The bands at 1634 , 1511 , and 1232 cm^{-1} were relative to Amide I, Amide II, and Amide III vibrations, respectively. Amide I vibration coincided with C=O stretching vibration and with a small contribution from N–H scissoring vibration.

The band of Amide II vibration included two components relative to C–N stretching and N–H wagging vibrations, while the two components relative to the band of Amide III were N–H twisting vibration and C–N stretching vibration with a contribution from O=C–N bending vibration. The absorbance band at 930 cm^{-1} could be attributed to the O=C–N vibration of Amide IV.

The FT-IR spectra of untreated hair after the irradiation of the three parts considered (the upper, central, and lower parts) were also recorded.

Irradiation can cause damage to the hair at a molecular level. From the spectrum reported in Figure 1b, recorded in the central part, a variation was noted in the amide region, and the absorption bands increased as a function of the increase in the S=O stretching of cysteic acid (1075 cm^{-1}).

The spectra of the three conditioners containing 1% active ingredient used for hair treatment compared with those of the conditioner without active ingredients (control) and with that of the pure active ingredient were subsequently recorded (Figure S1).

As can be seen from the figures, it was difficult to identify the peaks of the assets employed. The characterization of product traces on the hair was difficult due to the strong absorption of the hair. Their bands overlapped with those of the applied products. Therefore, the application of the conditioner on the hair, followed by rinsing, did not allow the identification of the individual active ingredients contained in the conditioner. Moreover, it was possible to detect the peaks of the conditioner (control) applied to the hair, even after rinsing. In fact, in Figure 2, the peaks related to the silicone contained in the formula could be identified (the absorption at $1039.9\text{--}1094\text{ cm}^{-1}$ was due to the silicone oil). The silicone derivative inside the cosmetic formulation involved an interaction with the S=O bond of the hair protein [44].

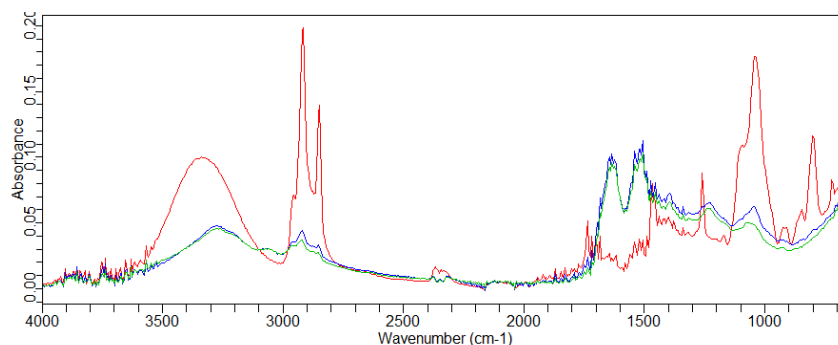


Figure 2. Overlay of the FT-IR spectra of the control conditioner (—) and the hair's central part: untreated (—) and treated with control conditioner (—).

The hair was treated with the pure active ingredients. The acquired spectra are shown in Figures 3, S2 and S3. A greater affinity for hair was found for GX-N. The presence of the characteristic peaks of the active ingredients could be observed at 2922 cm^{-1} , 2851 cm^{-1} , and 1071 cm^{-1} (Figure 3).

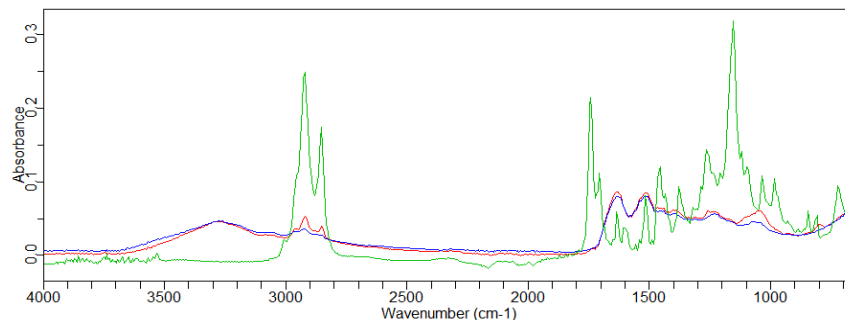


Figure 3. Overlay of the FT-IR spectra of GX-N (—) and the hair's central part: untreated (—) and treated with GX-N (—).

The comparison between the irradiated and not-irradiated hair treated with the control conditioner showed an increase in the absorbance of the amide peaks, while in the conditioner containing the 1% rice germ oil GX-N, the peaks of the amides had the same intensity as those of the non-irradiated hair, thus highlighting a protective effect on the hair due to this active ingredient (Figure 4).

3.2. SEM Analysis

This analysis allowed the evaluation of the morphological characteristics of the hair (the surface and the inner part through the cross-section) that could be influenced by cosmetic treatments (shampooing, conditioning, dyeing, bleaching, etc.) [5,47–49].

SEM images acquired on the three parts of the hair (upper, central, and lower) and for hair that was untreated, treated with control conditioner, and treated with conditioners containing 1% rice germ oil GX-N, 1% riceterol esters, and 1% rice germ oil PRO-15 are reported in Figures 5 and 6 and in the Supplementary Materials (Figures S4–S9).

The untreated hair showed a smooth surface. The layers of the cuticle were overlapped with irregularly contoured edges. In the lower part the surface appeared less smooth, and the edges were slightly raised. The treatment with the conditioners caused a change in the surface characteristics of the hair. The cuticle was rougher with more raised edges after the control conditioner treatment.

A deposit of the product was observed in the image of the hair treated with the conditioner GX-N. The edges of the scales of the hair appeared more low cut in comparison with the untreated hair (Figures 5, S4 and S5).

The images of the hair treated with conditioners containing 1% rice germ oil PRO-15 and 1% riceterol esters showed in the upper part an improvement of the surface characteristics in comparison with the control conditioner (Figure S4). The treatment with conditioner containing RSEs seemed better: the surface appeared smooth, and the edges of the cuticle were well overlapped.

Also in the central part, the application of the conditioner with RSEs produced a better effect than the conditioner containing PRO-15, and both were better than the reference (control). The images were very similar to those of the untreated hair (Figure 5).

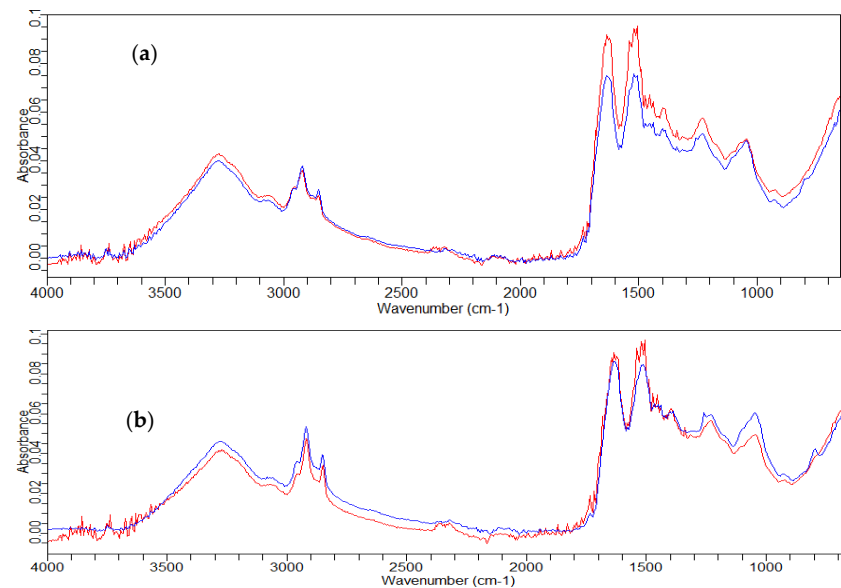


Figure 4. FT-IR spectra of the hair's central part. (a) Treated with control conditioner: — not irradiated; — irradiated. (b) Treated with conditioner GX-N: — not irradiated; — irradiated.

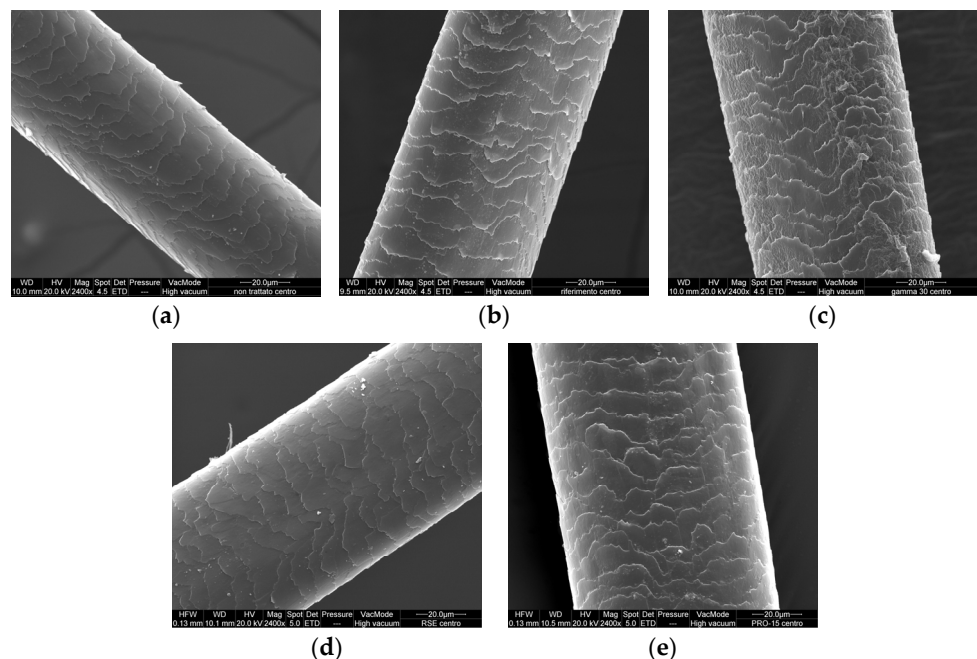


Figure 5. SEM images of hair's central part: (a) untreated, (b) treated with control conditioner, (c) treated with conditioner GX-N, (d) treated with conditioner RSE, and (e) treated with conditioner PRO-15.

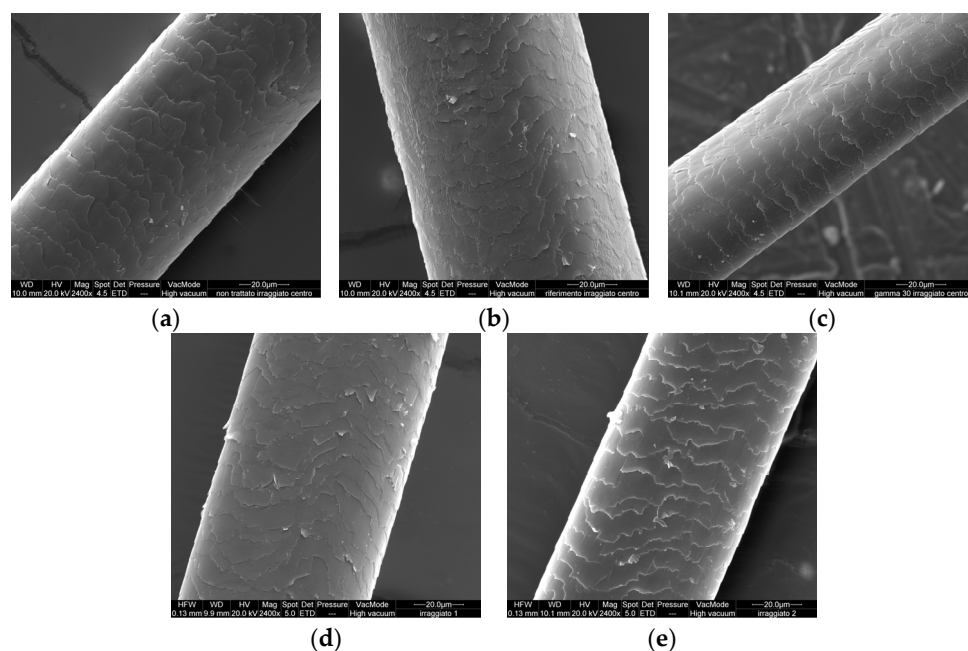


Figure 6. SEM images of irradiated hair's central part: (a) untreated, (b) treated with control conditioner, (c) treated with conditioner GX-N, (d) treated with conditioner RSE, and (e) treated with conditioner PRO-15.

In the lower part (Figure S5) the raised scales were more evident, especially in the hair treated with the reference (control). Both riceterol esters and rice germ oil PRO-15 improved the hair above all, in comparison with the treatment with the control but also compared with the untreated hair, which had some slightly raised scales. This effect was most noticeable in the lower part of the hair, which turned out to be the most damaged.

In the cross-section it was evident that the treatment of the hair with the reference (control) presented necklines of the cuticle compared with the inner part of the hair (cortex), which was less compact. The treatments with conditioners containing the active riceterol esters and rice germ oil PRO-15 had a positive effect on improving the cuticle adhesion and firmness (Figure S6).

In the images of the knotted not-irradiated hair, it could be observed that the treatment with the conditioner GX-N improved the morphology, especially in the bending, in which there was a greater uniformity and adhesion of the scales compared with the hair treated with the control conditioner and especially compared with the untreated hair (Figure S7). In the knotted hair, the treatment with the conditioner RSE seemed to provide the best results, as could be seen from the images relating to the narrowest part of the node (Figure S7).

With regard to the irradiated hair, a positive effect was found for hair treated with the conditioner GX-N. The cuticle maintained its structure with a regular overlap; the edges were not very jagged and slightly raised. The scales of the hair were more compact in comparison with both the hair treated with control conditioner and the untreated hair. This was more highlighted in the image relative to the central part of the hair (Figure 6).

In the untreated hair the edges of the cuticle were jagged and slightly raised with a less regular overlap. In the hair treated with the control conditioner, the cuticle had an irregular overlap with jagged edges.

Any positive effect was noted in the images relating to the hair treated with the conditioner containing the active riceterol esters or rice germ oil PRO-15; in other words, the effectiveness was poor. In the hair treated with the conditioner RSE the appearance was similar to that of the hair treated with the control conditioner, but the cuticle seemed more damaged. In the hair treated with the conditioner PRO-15, the surface appeared rough with more raised edges (Figure 6).

In the images of the cross-section of the hair (Figure S8), no substantial differences were observed with respect to those acquired for the non-irradiated samples.

In the images of the knotted irradiated hair we can see the positive effect of the application of the conditioner GX-N in comparison with both the control conditioner and the irradiated untreated hair (Figure S9). On the other hand, the effect of the treatment with the conditioner containing RSEs or PRO-15 appeared negative: the scales were more raised.

From the SEM images of the hair treated with the conditioners containing the three active ingredients under study, an improvement in the morphology of the hair was highlighted above all in the presence of RSE. It provided for a greater adhesion of the scales in all three parts (the distal, central, and proximal parts), making the surface smoother. With regard to the images obtained after irradiation, we can say that the positive effect of the application of the conditioner containing the active ingredient was present only in the case of rice germ oil GX-N with respect to both untreated hair and hair treated with the control conditioner.

3.3. Stress–Strain Test

In order to discuss the stress–strain test we must remember that the hair is a fiber with a complex, filamentous structure, composed of keratin, a fibrous protein rich in amino acids, in particular cysteine. These hair fibers undergo a stress when subjected to tensile forces, as in stylist and combing treatments, and for this reason the mechanical properties of the hair have been studied. For example, theoretical models have been proposed to interpret the stress–strain curves of wool fibers or of other α -keratin fibers [50–52]. The diameter of the hair is not constant but varies along the length of the hair, so the stress–strain is not uniform throughout the hair, but it can undergo variations.

Tensile properties are whole-fiber properties. They are evaluated via the load elongation (stress–strain) method, using a classical device generally called an extensometer (e.g., the Instron Tensile Tester). The stress–strain test involves stretching a fiber of a known length at a fixed rate in different environments. When the hair fiber is stretched, a stress–strain curve is obtained, which shows three distinct regions where the response of the hair to the applied stress is different (Figure 7).

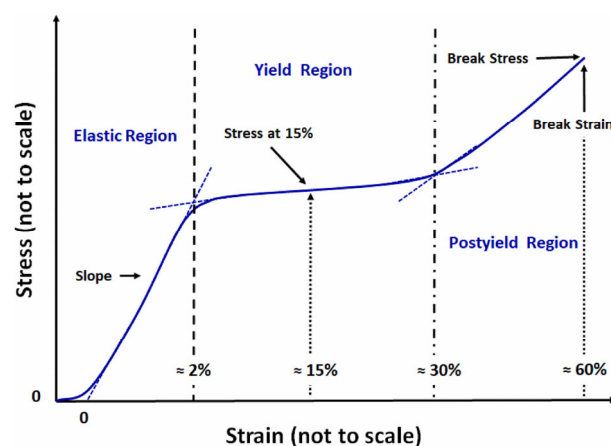


Figure 7. Stress–strain curve [52] Reprinted/adapted with permission from Ref. [52]. 2023, Elsevier.

The three abovementioned regions are as follows:

The first region is approximately between 0% and 2–3% of elongation. In this part of the curve the strain is almost proportional to the stress applied. The hair behaves like an elastic material; hence, this region is named the Hookean region.

The second region is between 2–3% and 25–30% of elongation. In this part, the strain increases very rapidly without noticeable changes in the stress applied. This area is called the yield region. In this region, the hair behaves like a liquid or an almost perfectly plastic material.

The third region is above 30% of elongation. As can be seen from the graph, the strain and the stress become again proportional. The hair behaves like an elastic solid before the final breakage [5].

In the Hookean part, when the hair fiber is stabilized in the dry state, the macroscopic elongation is mainly attributable to the hydrogen and salt bonds. Through the yield region the amount of β -keratin increases according to several studies on wool, which recognized a transformation of the α -keratin to β -keratin. At the end of this region, almost one-third of the keratin is in the β -structure [50,51].

Beyond 30% of elongation, in the post-yield region, the resistance to strain is controlled by covalent bonds and more specifically by disulfide linkage. After this region, the breakage of the hair fiber occurs [49,50].

Our new approach was based on the use of a dynamometer with a constant increase in extension, generally used for the evaluation of textile fiber tenacity, instead of the traditional Instron tensile tester. The results obtained are shown in Table 1 and in Figure 8.

Table 1. Stress–strain test results: diameter, extension, breaking point force, linear mass (Tex), and tenacity.

Sample	Diameter (μm)	Extension (%)	Breaking Point Force (cN)	Tex	Tenacity (cN/Tex)
NT hair	80.00 \pm 11.32	55.77 \pm 13.29	56.33 \pm 17.61	6.69	8.41 \pm 1.18
NTI hair	88.57 \pm 12.95	57.15 \pm 7.49	72.35 \pm 15.82	8.23	8.98 \pm 0.97
Hair with conditioner C	84.69 \pm 8.67	60.71 \pm 6.83	66.70 \pm 14.31	7.44	8.96 \pm 0.81
I hair with conditioner C	81.20 \pm 10.14	53.80 \pm 5.76	65.18 \pm 11.67	6.88	9.68 \pm 1.15
Hair with conditioner GX-N	88.80 \pm 8.08	60.53 \pm 5.59	69.35 \pm 7.83	8.02	8.64 \pm 1.14
I hair with conditioner GX-N	89.24 \pm 7.07	60.21 \pm 5.84	70.65 \pm 17.24	8.25	8.56 \pm 1.53
Hair with conditioner RSE	89.87 \pm 8.52	64.52 \pm 5.53	69.90 \pm 17.53	8.38	8.56 \pm 2.36
I hair with conditioner RSE	85.69 \pm 7.07	57.65 \pm 4.32	74.28 \pm 20.24	7.72	9.76 \pm 13.25
Hair with conditioner PRO-15	82.99 \pm 10.77	62.92 \pm 8.03	63.98 \pm 14.03	7.20	9.16 \pm 1.80
I hair with conditioner PRO-15	81.73 \pm 7.66	55.94 \pm 4.73	67.55 \pm 13.63	6.93	9.84 \pm 1.38

NT: not treated; NTI: not treated irradiated; C: control; I: irradiated.

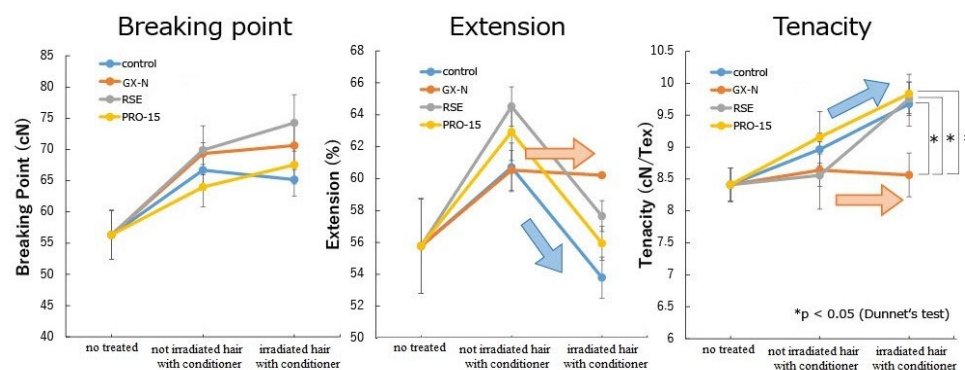


Figure 8. Stress–strain results: breaking point, extension, and tenacity.

The standard deviations detected in all cases were very likely due to the variations in the diameter of the hair used.

The application of the conditioners, in particular the conditioner RSE, leads to a greater extension than in untreated hair. Significant differences were observed in the hair treated with the conditioners RSE ($p = 0.01$) and PRO-15 ($p = 0.046$). This could be due to their greater penetrating properties, which cause the hair to be softer and more capable of being deformed.

The extension in the untreated hair after irradiation did not show any significant variation. On the other hand, the extension was reduced in the hair treated with conditioners. Only the hair treated with the conditioner GX-N preserved the same lengthening before and after irradiation, while the comparison between the non-irradiated and irradiated hair

showed significant differences in the hair treated with the control conditioner ($p = 0.001$), with the conditioner RSE ($p = 9.1 \times 10^{-5}$) and with the conditioner PRO-15 ($p = 0.002$).

Significant differences were not observed between the untreated irradiated hair and the irradiated hair treated with the various conditioners. However, the extension increased in the hair treated with the conditioner GX-N, it decreased with the control conditioner and with the conditioner PRO-15, and it did not change with the conditioner RSE.

The comparison of irradiated hair treated with the control conditioner and the hair treated with the conditioners containing the active ingredients showed significant differences with GX-N ($p = 0.001$) and RSEs ($p = 0.02$).

The application of conditioners containing rice germ oil GX-N, rice germ oil PRO-15, and riceterol esters led to an increase in the breaking point force as compared with the untreated hair. Thus, the three active ingredients strengthened the hair and determined an increase in the resistance to breakage before irradiation. After irradiation, an increase in the breaking point force could be observed for the untreated hair and for the hair treated with the conditioners RSE and PRO-15, while it remained almost unchanged for the hair treated with the control conditioner and with the conditioner GX-N. The difference was significant only for the untreated hair ($p = 0.0044$).

With regard to the tenacity, no significant differences were observed between the untreated hair and hair treated with the various conditioners and between the hair treated with the control conditioner and the hair treated with the conditioners containing the active ingredients. As for the breaking point force, the tenacity varied according to the diameter of the hair.

After irradiation its value was higher in all cases except that for the conditioner GX-N. The comparison of the tenacity values obtained before and after irradiation showed significant differences between the hair treated with the control conditioner ($p = 0.03$) and the hair treated with the conditioner RSE ($p = 0.05$).

Irradiation did not cause statistically detectable variations in the sample treated with the conditioner GX-N, which maintained the same values before and after irradiation. These values were not significantly different from those found for the untreated, non-irradiated hair, while the differences were significant between the untreated irradiated hair and the irradiated hair treated with the control conditioner ($p = 0.05$), with the conditioner RSE ($p = 0.03$), and with the conditioner PRO-15 ($p = 0.03$). Furthermore, after irradiation, the comparison between the hair treated with the control conditioner and the hair treated with the other conditioners showed a significant difference only with the conditioner GX-N ($p = 0.01$).

These results confirmed the data obtained for the elongation and the breaking point. A higher linear mass (Tex) and tenacity could provide the hair greater stiffness and therefore a reduction in its deformation. This could derive from the difficulty, following irradiation, of the transformation of keratin from the α to the β form [53]. Exposure to UV radiation can lead to a decrease in the lipid content and an increase in the water loss with a consequent reduction in the plasticity of the hair matrix [54]. Water is a strong plasticizer of hair. Its solvation causes the breaking of hydrogen bonds and salt bridges within the protein structure, which results in an increase in the flexibility of the fiber. The plasticizing effect of water leads to an increase in the extension before reaching the breaking point [53].

The irradiation in the case of the hair treated with the conditioner GX-N did not change the extension (%), the breaking point force, and the tenacity, thus indicating a stability of the hair structure.

The application of the conditioner GX-N implied a stability to UV irradiation.

According to the values obtained from the stress–strain test, the hair treated with the conditioner GX-N offered the best protection with regard to irradiation; thus, a confirmation of this fact has been verified by evaluating the hair protection factor (HPF).

3.4. Hair Protection Factor

The hair, as the skin, must to be protected from damage induced by solar radiation. The natural photoprotection of the hair is provided by melanin, in particular by eumelanin, which is also an endogenous photoprotector of the skin. Unpigmented hair, such as gray and white hair, is more susceptible to UV damage than pigmented hair [4]. Melanin granules are located in the cortex of the fiber but not in the cuticle, and consequently, the natural pigment protects the internal part of the fiber but not the external cuticle [4]. Thus, it appears important to have ingredients in hair care products that, by depositing themselves on the surface of the hair, protect the cuticle and consequently the whole fiber. The protective capacity of the ingredient under study was evaluated by determining the HPF value based on the variation in the tensile properties.

The HPF values determined by applying the Nacht formula were as follows:

$$\text{HPF}(\text{GX} - \text{N}) = \frac{(0.0101 - 0.0040)}{(0.0060 - 0.0045)} = 4.06$$

$$\text{HPF}(\text{RSE}) = \frac{(0.0101 - 0.0040)}{(0.0065 - 0.0046)} = 3.21$$

$$\text{HPF}(\text{PRO} - 15) = \frac{(0.0101 - 0.0040)}{(0.0099 - 0.0075)} = 2.54$$

On an arbitrary scale of HPF from 0 to 15 corresponding to a protection (%) ranging from 0 to 100, the found HPF values corresponded approximately to 27% protection in the case of hair treated with the conditioner GX-N, to 17% protection with the conditioner PRO-15, and to 21.4% with the conditioner RSE with respect to the untreated hair, as can be extrapolated from the graphic proposed by Nacht [2].

The HPF values corresponded to low protection in the case of rice germ oil PRO-15 and riceterol ester and to medium–low protection in the case of rice germ oil GX-N. However, it must be considered that in the formulation, there were not sunscreens, and therefore, these values were appreciable. The active substances could have a booster effect in association with sunscreens. Clearly, a greater contribution will be made by the rice germ oil GX-N.

3.5. Polarized Light Microscopy Analysis

Polarized light analysis is a new and innovative method of evaluation, even if it has been known for a long time, but it has not yet been much investigated in relation to hair care. Polarized light microscopy, which is a traditional technique in mineralogy, has also become an undisputed useful diagnostic in the trichological field [43,55–58].

Keratin, the sequential, repetitive, and crystalline protein, has the property of birefringence and the ability to retard the wave of polarized light (also called retardance) passing through the hair that at the microscope appears bright and colored on the black background [43]. There are two types of wave retards: (a) the first, visible as a color and called the “polarization color”, is due to the thickness of the keratin, and according to the Newton scale, each color is connected to a precise diameter; (b) the second wave retard, due to the crystallographic orientation and to the pigment contained in the keratin, is called the “compensation color”. In mineralogy, each visible color is associated to a specific structural and molecular order; in trichology this relation is considered connected with the crystallographic structure of the hair, that is, to its “quality”. The colors visible through a microscope in polarized light, therefore, provide certain data for evaluations that otherwise would only be conceivable [59,60].

The polarized light microscopy provides the right information that provides a safely targeted and calibrated approach to the professional cosmetics field, especially with respect to the use of products that bring chemical–physical modifications to the keratin of the hair.

The preparation of the samples for the analysis is simple and fast. The technique is not invasive, and it is appealing and immediately applicable; the procedure, however,

presupposes a thorough knowledge of microscopy and trichology, as well as a good practical experience [55].

In trichological polarized light microscopy the size of the wave retard, and therefore the color we read from the hair analysis, results from the thickness of the hair itself. Observing several keratinic materials with various/different diameters at the microscope, we observed the following colors: white to yellow up to 50 μm , red between 50 and 70 μm , and blue between 70 and 90 μm (the overlapping of the pure colors blue and red led to magenta). From 90 μm on we observed very important wave retards, and we passed from blue, darker and darker blue, to green (Figure 9). Clearly, it must be noted that any extraneous body present in the keratinic structure produced wave retards and changes in the nuances of the color and moved the bands toward darker colors. If the material inserted inside the structure rearranged or added keratin, a recovery or an increase in the polarization colors was observed [59,60].

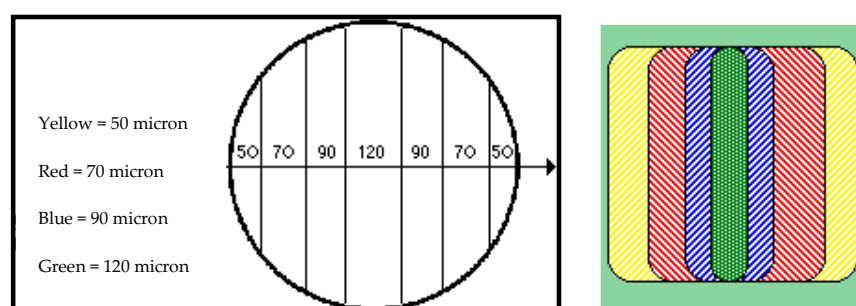


Figure 9. Polarization colors and hair diameter relationships.

In the following are reported the observations relative to the samples analyzed by polarized light microscopy. The original natural untreated hairs had a good organization of the keratin; the external layer of the cuticle, colored in yellow, and the cortex, uniformly colored in ochre, were visible. After irradiation, the hair did not have an optimal keratin structure, but it was moderately unstructured (Figure S10); the hair had a light ochre color, and the cuticle was slightly highlighted. The hair treated with the control conditioner had a mediocre keratin organization; the cuticle had a lower thickness, and the cortex had a not-homogeneous light ochre color. After irradiation the structure of the keratin appeared slightly compromised. The hair was uniformly yellow, and the separation between the cuticle and the cortex was not highlighted (Figure S11). The hair treated with the conditioner GX-N had a good keratin organization. The treatment, in addition to improving the polarization colors, provided better evidence of the cuticular area, which suggested a deposit of the active ingredient on this portion of the hair. After irradiation, no substantial variations were highlighted (Figure 10). The hairs treated with the conditioners RSE and PRO-15 had a fairly good keratin organization; the hair appeared similar to the untreated hair with a clearly visible yellow cuticle but with a lighter ochre colored cortex. After irradiation, with the conditioner PRO-15 the yellow colored cuticle layer was clearly visible (Figure S12), while in the case of the conditioner RSE, the thickness of the cuticle was reduced (Figure S13).

From the analyses carried out with the polarized light microscope it can be seen that the conditioners containing the active ingredients resulted in polarization colors compatible with the diameter of the hair and improved with respect to the control conditioner. The active ingredients acted mainly on the cuticular portion rather than on the cortex. The same effect could also be observed on irradiated hair where GX-N was confirmed to be the most effective.

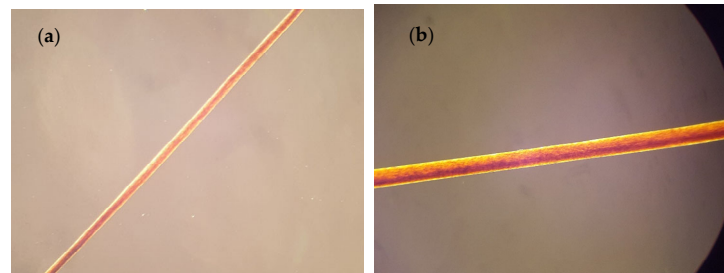


Figure 10. Polarized light microscopy images of hair treated with conditioner GX-N: (a) non irradiated and (b) irradiated.

4. Conclusions

The consumers of hair care products are very careful in choosing products, in terms of both their composition and their effectiveness. Therefore, the availability of methods and tests for evaluating the efficacy of the products appears to be very crucial.

In this study the effectiveness of three active substances (rice germ oil GX-N, rice germ oil PRO-15, and riceterol esters) included in hair conditioners was evaluated through different methodologies.

The applied techniques allowed us to highlight changes in the properties of the hair in the presence of the conditioners with the active ingredients with respect to the reference conditioner. This was an interesting result considering that the product was in contact with the hair only for a short time, and then it was rinsed off. The different analyses performed provided consistent data indicating the presence of a localized effect on the cuticular portion level of the hair.

The active ingredients showed good efficacy in improving the surface and mechanical properties of the hair. This fact was further confirmed through the comparison with the control conditioner, which in some cases caused negative effects.

The conditioners containing the active ingredients restored the morphological properties of the hair, making the surface smoother. In particular, riceterol esters showed good properties when applied to the normally more damaged distal part of the hair. Rice germ oil GX-N significantly improved the photoprotection. This effect may have been due to two factors: (i) its higher γ -oryzanol content, probably responsible for the higher HPF value, and (ii) its greater affinity for the hair and the building of a deposit on the surface of the cuticle as shown by FT-IR, SEM, and polarized light microscopy analyses.

In conclusion, the used methodologies were found to be suitable for establishing the effectiveness that the studied rice derivatives had on the hair. In turn, these results broaden the range of applications of these ingredients in hair care products, as well as in skin products.

Supplementary Materials: The following supporting information can be downloaded at <https://www.mdpi.com/article/10.3390/cosmetics10060163/s1>: Figures S1–S3: FT-IR spectra; Figure S1: FT-IR spectra of the active ingredients and the four conditioners; Figure S2: FT-IR spectra of PRO-15 and the untreated and treated hair; Figure S3: FT-IR spectra of RSEs and the untreated and treated hair. Figures S4–S9: SEM images of untreated hair and hair treated with conditioners; Figure S4: hair's upper part; Figure S5: hair's lower part; Figure S6: hair section; Figure S7: knotted hair; Figure S8: irradiated hair section; Figure S9: irradiated knotted hair. Figures S10–S13: Polarized light images of non-irradiated and irradiated hair; Figure S10: untreated hair; Figure S11: hair treated with control conditioner; Figure S12: hair treated with conditioner PRO-15; Figure S13: hair treated with conditioner RSE.

Author Contributions: Conceptualization, C.A. and M.C.; methodology, G.S., F.F. and T.O.; validation, M.C., G.S. and T.O.; investigation, G.S. and F.F.; data curation, C.A., F.T. and M.C.; writing—original draft preparation, C.A. and M.C.; writing—review and editing, C.A., F.T., M.C. and T.O.; supervision, C.A. and F.T. All authors have read and agreed to the published version of the manuscript.

Funding: This research was funded by Tsuno Rice Fine Chemical Co., Ltd.

Institutional Review Board Statement: Not applicable.

Informed Consent Statement: Not applicable.

Data Availability Statement: The data presented in this study are all available within the article and Supplementary Materials.

Acknowledgments: The authors wish to thank Silvia Cianchi (Istituto G. Palloni, Montevarchi, Arezzo, Italy) for the use of the polarized light microscopy.

Conflicts of Interest: The authors declare no conflict of interest. The companies (Unicosmesi Srl, FEELCOSMETIC S.R.L. and Tsuno Rice Fine Chemical Co., Ltd.) had no influence on the design of the study and on the collection and analyses of data. In addition, all authors declare that the results of the study are presented clearly, honestly, and without fabrication, falsification, or inappropriate data manipulation.

References

1. Robbins, C.R. *Chemical and Physical Behavior of Human Hair*, 4th ed.; Springer: New York, NY, USA, 2001.
2. Nacht, S. Sunscreens and Hair. *Cosmet. Toilet.* **1990**, *105*, 55–60.
3. De Galvez, M.V.; Aguilera, J.; Bernabò, J.L.; Sánchez-Roldán, C.; Herrera-Ceballos, E. Human Hair as a Natural Sun Protection Agent: A Quantitative Study. *Photochem. Photobiol.* **2015**, *91*, 966–970. [[CrossRef](#)]
4. Dario, M.F.; Baby, A.R.; Velasco, M.V.R. Effects of solar radiation on hair and photoprotection. *J. Photochem. Photobiol. B Biol.* **2015**, *153*, 240–246. [[CrossRef](#)] [[PubMed](#)]
5. Velasco, M.V.R.; Dias, T.S.C.; Freitas, A.Z.; Viera Junior, N.D.; Pinto, C.A.S.O.; Kaneko, T.M.; Baby, A.R. Hair fiber characteristics and methods to evaluate hair physical and mechanical properties. *Braz. Pharm. Sci.* **2009**, *45*, 153–162. [[CrossRef](#)]
6. Botelho Laurengo, C.; Masquetti Fava, A.L.; Mendes dos Santos, E.; Malvezzi de Macedo, L.; Lacalendola Tundisi, L.; Artem Ataide, J.; Gava Mazzola, P. Brief description of the principles of prominent methods used to study the penetration of materials in to human hair and a review of examples of their use. *Int. J. Cosmet. Sci.* **2021**, *43*, 113–122. [[CrossRef](#)] [[PubMed](#)]
7. Da Gama, R.M.; Baby, A.R.; Velasco, V.R. In vitro methodologies to evaluate the effects of hair care products on hair fiber. *Cosmetics* **2017**, *4*, 2. [[CrossRef](#)]
8. Lichtman, J.W.; Conchello, J.A. Fluorescence microscopy. *Nat. Methods* **2005**, *2*, 910–919. [[CrossRef](#)]
9. Tinoco, A.; Gonçalves, J.; Silva, C.; Laureiro, A.; Gomes, A.C.; Cavaco-Paulo, A.; Ribeiro, A. Keratin-based particles for protection and restoration of hair properties. *Int. J. Cosmet. Sci.* **2018**, *40*, 408–419. [[CrossRef](#)] [[PubMed](#)]
10. Chen, G.; Ji, C.; Collins, L.Z.; Hoptroff, M.; Jassen, H.G. Visualization of zinc pyrithione particles deposited on the scalps from a shampoo by tape-strip sampling and scanning electron microscopy/energy dispersive X-ray spectroscopy measurement. *Int. J. Cosmet. Sci.* **2018**, *40*, 530–533. [[CrossRef](#)] [[PubMed](#)]
11. Takashi, T. A highly resistant structure between the cuticle and the cortex of human hair III: Characterization of the structure CARB. *Int. J. Cosmet. Sci.* **2021**, *43*, 254–262. [[CrossRef](#)] [[PubMed](#)]
12. Grasvenor, A.J.; Deb-Choudhury, S.; Middlewood, P.G.; Thomas, A.; Lee, E.; Vernon, J.A.; Woods, J.L.; Taylor, C.; Bell, F.I.; Clerens, S. The physical and chemical disruption of human hair after bleaching-studies by transmission electron microscopy and redox proteomics. *Int. J. Cosmet. Sci.* **2018**, *40*, 536–548. [[CrossRef](#)] [[PubMed](#)]
13. McMullen, R.L.; Zhang, G. Investigation of the internal structure of human hair with atomic force microscopy. *J. Cosmet. Sci.* **2020**, *71*, 117–131.
14. Seshadri, I.P.; Bhushan, B. Effect of ethnicity and treatments on in situ tensile response and morphological changes of human hair characterized by atomic force microscopy. *Acta Mater.* **2008**, *56*, 3585–3597. [[CrossRef](#)]
15. Pavani, C.; Severino, D.; Villa Dos Santos, N.; Chiarelli-Neto, O.; Baptista, M.S. Spectroscopy as a tool to evaluate hair damage and protection. *Int. J. Cosmet. Sci.* **2018**, *40*, 596–603. [[CrossRef](#)] [[PubMed](#)]
16. Ryu, S.R.; Jang, W.; Yu, S.I.; Lee, B.H.; Kwon, O.S.; Shin, K. FT-IR Microspectroscopic Imaging of Cross-Sectioned Human Hair during a Bleaching Process. *J. Cosmet. Dermatol. Sci. Appl.* **2016**, *6*, 181–190. [[CrossRef](#)]
17. Kuzuhara, A. Internal structural changes in keratin fibers resulting from combined hair waving and stress relaxation treatments: A Raman spectroscopic investigation. *Int. J. Cosmet. Sci.* **2016**, *38*, 201–209. [[CrossRef](#)] [[PubMed](#)]
18. Grundman, C.B. Investigating prevention of UV damage to hair using Raman spectroscopy. *J. Cosmet. Sci.* **2018**, *69*, 357–362.
19. Kuzuhara, A. Raman spectroscopic of L-phenylalanine and hydrolyzed eggwhite protein into keratin fibers. *J. Appl. Polym. Sci.* **2011**, *122*, 2680–2689. [[CrossRef](#)]
20. Scanavez, C.; Zoega, M.; Barbosa, A.; Joekes, I. Measurement of hair luster by diffuse reflectance spectrophotometry. *J. Cosmet. Sci.* **2000**, *55*, 289–302.
21. Haake, H.M.; Lagranè, H.; Brands, A.; Eisfeld, W.; Melchior, D. Determination of the substantivity of emollients to human hair. *J. Cosmet. Sci.* **2007**, *58*, 443–450.
22. Evans, A.O.; Marsh, J.M.; Wickett, R.R. The uptake of water hardness metal by human hair. *J. Cosmet. Sci.* **2011**, *62*, 383–391.

23. Lima, C.R.R.; Almeida, M.M.; Velasco, M.V.R.; Matos, J.R. Thermoanalytical characterization study of hair from different ethnicities. *J. Therm. Anal. Calorim.* **2016**, *123*, 2321–2328. [[CrossRef](#)]
24. Da Gama, R.M.; Balagh, T.S.; França, S.; Sà-Dias, T.C.; Bedin, V.; Baby, A.R.; Velasco, M.V.R. Thermal analysis of hair treated with oxidative hair dye under influence of conditioners agents. *J. Therm. Anal. Calorim.* **2011**, *106*, 339–405. [[CrossRef](#)]
25. Wortmann, F.J.; Springob, C.; Sendelbach, G. Investigations of cosmetically treated human hair by different scanning calorimetry in water. *J. Cosmet. Sci.* **2002**, *53*, 219–228. [[PubMed](#)]
26. Blanco, B.; Durost, B.; Myers, R. Gel permeation chromatography: An effective method of quantifying the adsorption of cationic polymers by bleached hair. *J. Soc. Cosmet. Chem.* **1997**, *48*, 127–131.
27. Mintz, G.R.; Reinhart, G.M.; Lent, B. Relationship between collagen hydrolysate molecular weight and peptide substantivity hair. *J. Soc. Cosmet. Chem.* **1991**, *42*, 35–44.
28. McMullen, R.L.; Scless, T.; Kulcsar, L.; Foltis, L.; Gillece, T. Evaluation of the surface properties of hair with acoustic emission analysis. *Int. J. Cosmet. Sci.* **2021**, *43*, 88–101. [[CrossRef](#)] [[PubMed](#)]
29. Puccetti, G.; Kulcsar, L. Hair surface quality: Laser scattering as a tool for characterizing the surface condition and deposits from shampoo and conditioners. *Int. J. Cosmet. Sci.* **2020**, *42*, 89–98. [[CrossRef](#)]
30. New, S.; Daniels, G.; Gummer, C.L. Measuring the frequency of consumer hair combing and magnitude of combing forces on individual hairs in a tress and the implications for product evaluation and claims substantiation. *Int. J. Cosmet. Sci.* **2018**, *40*, 461–466. [[CrossRef](#)] [[PubMed](#)]
31. Burlando, B.; Cornara, L. Therapeutic properties of rice constituted and derivatives (*Oryza sativa* L.): A review update. *Trends Food Sci. Technol.* **2014**, *40*, 82–98. [[CrossRef](#)]
32. Punia, S.; Kumar, M.; Siroha, A.K.; Purewal, S.S. Rice Bran Oil: Emerging Trends in Extraction, Health Benefit, and Its Industrial Application. *Rice Sci.* **2021**, *28*, 217–232. [[CrossRef](#)]
33. Garba, U.; Singanusong, R.; Jiamyangyuen, S.; Thongsook, T. Extraction and utilization of rice bran oil: A review extraction and utilization of rice bran oil. In Proceedings of the 4th International Conference on Rice Bran Oil 2017 (ICRBO 2017). Rice Bran Oil Application: Pharma-Cosmetics, Nutraceuticals and Food, Bangkok, Thailand, 24–25 August 2017.
34. Manosroi, A.; Ruksiriwanich, W.; Abe, M.; Sakai, H.; Manosroi, W.; Manosroi, J. Biological activities of the rice bran extract and physical characteristics of its entrapment in niosomes by supercritical carbon dioxide fluid. *J. Supercrit. Fluids* **2010**, *54*, 137–144. [[CrossRef](#)]
35. Hashemi, K.; Pham, C.; Sung, C.; Mamaghani, T.; Juhasz, M.; Mesinkovska, N.A. Systematic Review: Application of Rice Products for Hair Growth. *J. Drugs Dermatol.* **2022**, *21*, 177–185. [[CrossRef](#)]
36. Choi, J.S.; Jeon, M.H.; Moon, W.S.; Moon, J.N.; Cheon, E.J.; Kim, J.W.; Jung, S.K.; Ji, Y.H.; Son, S.W.; Kim, M.R. In Vivo Hair Growth-Promoting Effect of Rice Bran Extract Prepared by Supercritical Carbon Dioxide Fluid. *Biol. Pharm. Bull.* **2014**, *37*, 44–53. [[CrossRef](#)] [[PubMed](#)]
37. Kim, I.H.; Kim, C.J.; You, J.M.; Lee, K.W.; Kim, C.T.; Chung, S.H.; Tae, B.S. Effect of Roasting Temperature and Time on the Chemical Composition of Rice Germ Oil. *J. Am. Oil Chem. Soc.* **2002**, *79*, 413–418. [[CrossRef](#)]
38. Kobayashi, M.; Nakagawa, S.; Nakamura, T.; Tsuno, T. Skin improvement effects of phytosterol ester derived from rice bran. *J. Food Sci. Nutr. Res.* **2023**, *6*, 17–23. [[CrossRef](#)]
39. Pawar, S.K.; Vavia, P.R. Rice germ oil as multifunctional excipient in preparation of self-microemulsifying drug delivery system (SMFDDS) of tacrolimus. *AAPS PharmSciTech* **2012**, *13*, 254–261. [[CrossRef](#)] [[PubMed](#)]
40. ISO 105-B02:2014; Textiles – Test for colour fastness – Part B02: Colour fastness to artificial light: Xenon arc fading lamp test. ISO: Geneva, Switzerland.
41. Bayak, R.; Meyer, C.F.; Kass, G.S. Elasticity and Tensile Properties of Human Hair. I Single Fiber Test Method. *J. Soc. Cosm. Chem.* **1969**, *20*, 615–626.
42. Bayak, R.; Meyer, C.F.; Kass, G.S. Elasticity and Tensile Properties of Human Hair. II. Light Radiation Effects. *J. Soc. Cosmet. Chem.* **1971**, *22*, 667–678.
43. Oldenbourg, R. Polarized light microscopy: Principles and practice. *Cold Spring Harb. Protoc.* **2013**, *2013*, pdb-top078600. [[CrossRef](#)]
44. Pienpinijthama, P.; Thammacharoen, C.; Naranitad, S.; Ekgasit, S. Analysis of cosmetic residues on a single human hair by ATR FT-IR microspectroscopy. *Spectrochim. Acta A Mol. Biomol. Spectrosc.* **2018**, *197*, 230–236. [[CrossRef](#)]
45. Boll, M.S.; Doty, K.C.; Wickenheiser, R.; Lednew, I.K. Differentiation of hair using ATR FT-IR spectroscopy: A statistical classification of dye and non dyed hairs. *Forensic Chem.* **2017**, *6*, 1–9. [[CrossRef](#)]
46. Cloete, K.J.; Smit, Z.; Gianoncelli, A. Multidimensional Profiling of Human Body Hairs Using Qualitative and Semi-Quantitative Approaches with SR-XRF, ATR FT-IR, DSC, and SEM-EDX. *Int. J. Mol. Sci.* **2023**, *24*, 4166. [[CrossRef](#)] [[PubMed](#)]
47. Chu, F.; Anex, D.S.; Jones, A.D.; Hart, B.R. Automated analysis of scanning electron microscopic images for assessment of hair surface damage. *R. Soc. Open. Sci.* **2020**, *7*, 191438. [[CrossRef](#)] [[PubMed](#)]
48. Bianchi, S.; Bernardi, S.; Continenza, M.A.; Vincenti, E.; Antonouli, S.; Torge, D.; Macchiarelli, G. Scanning Electron Microscopy Approach for Evaluation of Hair Dyed with *Lawsonia inermis* Powder: In vitro Study. *Int. J. Morphol.* **2020**, *38*, 96–100. [[CrossRef](#)]
49. Davis, C.; Khofar, P.N.A.; Karim, U.K.A.; Rashid, R.A.; Mahat, M.M.; Halim, M.I.A. Critical assessment on structural analysis of scalp hair using scanning electron microscope (SEM) and compound microscope. *Mater. Today Proc.* **2020**, *29*, 244–249. [[CrossRef](#)]

50. Hearle, J.W.S. A critical review of the structural mechanics of wool and hair fibers. *Int. J. Biol. Macromol.* **2000**, *27*, 123–138. [[CrossRef](#)]
51. Goldsmith, L.A.; Baden, H.P. The mechanical properties of hair I. The dynamic sonic modulus. *J. Investig. Dermatol.* **1970**, *55*, 256–259. [[CrossRef](#)] [[PubMed](#)]
52. Wortmann, F.J.; Quadflieg, J.M.; Wortmann, G. The information content of tensile tests of human hair (wet) is limited: Variables mainly cluster in just two principal components. *J. Mech. Behav. Biomed. Mater.* **2022**, *129*, 105145. [[CrossRef](#)]
53. Evans, T. Measuring Hair Strength-Part 1: Stress-Strain Curves. *Cosmet. Toilet.* **2013**, *128*, 590–594.
54. Coderch, L.; Alonso, C.; García, M.T.; Pérez, L.; Martí, M. Hair lipid structure: Effect of surfactants. *Cosmetics* **2023**, *10*, 107. [[CrossRef](#)]
55. Ferri, A.; Franzoia, R.; Martínez-Sánchez, G. Hair Analysis by Polarized Light Microscopy, a New Tool in Medical Research. *J. Toxicol. Cur. Res.* **2018**, *2*, 004. [[CrossRef](#)]
56. Adya, K.A.; Inamadar, A.C.; Palit, A.; Shivanna, R.; Deshmukh, N.S. Light Microscopy of the Hair: A Simple Tool to “Untangle” Hair Disorders. *Int. J. Trichol.* **2013**, *3*, 46–56. [[CrossRef](#)]
57. Valente, N.Y.S.; Machado, M.C.M.R.; Boggio, P.; Alves, A.C.F.; Bergonse, F.N.; Casella, E.; Vascelos, D.M.; Grumach, A.S.; de Oliveria, Z.N.P. Polarized light microscopy of hair shafts aids in the differential diagnosis of Chédiak-Higashi and Griscelli-Prunieras syndrome. *Clinics* **2006**, *61*, 327–332. [[CrossRef](#)]
58. Wallace, M.P.; de Berker, D.A. Hair diagnoses and signs: The use of dermatoscopy. *Clin. Exp. Dermatol.* **2010**, *35*, 41–46. [[CrossRef](#)]
59. Marliani, A.; Gigli, P.; Salin, M. Trichological microscopy in polarized light. *J. Eur. Acad. Dermatol. Venereol.* **1997**, *1001*, S126. [[CrossRef](#)]
60. Marliani, A.; Gigli, P.; Antognini, G.; Tartù, S.; Bini, F.; Agostinacchio, G. *Microscopia Tricologica in Luce Polarizzata*; Società Italiana di Tricologia: Firenze, Italy, 2015.

Disclaimer/Publisher’s Note: The statements, opinions and data contained in all publications are solely those of the individual author(s) and contributor(s) and not of MDPI and/or the editor(s). MDPI and/or the editor(s) disclaim responsibility for any injury to people or property resulting from any ideas, methods, instructions or products referred to in the content.